Front. Struct. Civ. Eng. 2019, 13(6): 1510–1519
https://doi.org/10.1007/s11709-019-0577-8

RESEARCH ARTICLE

Probabilistic seismic response and uncertainty analysis of continuous bridges under near-fault ground motions

Hai-Bin MA[a], Wei-Dong ZHUO[a*], Davide LAVORATO[b], Camillo NUTI[a,b], Gabriele FIORENTINO[b], Giuseppe Carlo MARANO[a,c], Rita GRECO[c], Bruno BRISEGHELLA[a]

[a] *College of Civil Engineering, Fuzhou University, Fuzhou 350108, China*

[b] *Department of Architecture, Roma Tre University, Roma 00154, Italy*

[c] *College of Civil Engineering and Architecture, Politecnico di Bari University, Bari 70126, Italy*

[*] *Corresponding author. E-mail: zhuowd@fzu.edu.cn*

ABSTRACT Performance-based seismic design can generate predictable structure damage result with given seismic hazard. However, there are multiple sources of uncertainties in the seismic design process that can affect desired performance predictability. This paper mainly focuses on the effects of near-fault pulse-like ground motions and the uncertainties in bridge modeling on the seismic demands of regular continuous highway bridges. By modeling a regular continuous bridge with OpenSees software, a series of nonlinear dynamic time-history analysis of the bridge at three different site conditions under near-fault pulse-like ground motions are carried out. The relationships between different Intensity Measure (IM) parameters and the Engineering Demand Parameter (EDP) are discussed. After selecting the peak ground acceleration as the most correlated IM parameter and the drift ratio of the bridge column as the EDP parameter, a probabilistic seismic demand model is developed for near-fault earthquake ground motions for 3 different site conditions. On this basis, the uncertainty analysis is conducted with the key sources of uncertainty during the finite element modeling. All the results are quantified by the "swing" base on the specific distribution range of each uncertainty parameter both in near-fault and far-fault cases. All the ground motions are selected from PEER database, while the bridge case study is a typical regular highway bridge designed in accordance with the Chinese Guidelines for Seismic Design of Highway Bridges. The results show that PGA is a proper IM parameter for setting up a linear probabilistic seismic demand model; damping ratio, pier diameter and concrete strength are the main uncertainty parameters during bridge modeling, which should be considered both in near-fault and far-fault ground motion cases.

KEYWORDS continuous bridge, probabilistic seismic demand model, Intensity Measure, near-fault, uncertainty

1 Introduction

The concept of performance-based seismic design (PBSD) [1,2] has been widely accepted by the researchers in current earthquake engineering research. This general design philosophy could focus on comprehensive performance objectives such as the structure's usability, safety, and economics [3]. On this basis, Pacific Earthquake Engineering Research (PEER) Centre developed a new-generation of performance-based earthquake engineering (PBEE) framework based on full probability theory, involving four generalized variables: the Intensity Measure (IM), the Engineering Demand Parameter (EDP), the Damage Measure (DM), and the Decision Variable (DV) [4–6]. Nevertheless, this seismic design procedure contains a large number of uncertainty parameters, such as seismic hazard, seismic demand, seismic capacity, and structure modeling. Once the performance level with given exceeding probability is ensured, the uncertainty in either seismic demand or capacity may significantly increase the realization cost [7]. Therefore, how to recognize and quantify the uncertainty parameter are important to push PBEE design theory into practical engineering application.

As for specific modeling uncertainty in engineering structures, previous studies have already recognized the

Article history: Received Aug 19, 2018; Accepted Dec 20, 2018

importance of modeling parameter uncertainty and developed appropriate methodologies for data quantification [8–10]. However, most of the seismic response analyses were mainly based on far-fault earthquake ground motions.

Pan et al. [11] studied 10 typical continuous bridge samples of New York State by Latin Hypercube sampling method and restricted pairing approach. Uncertainties associated with the material strength, bridge mass, friction coefficient of bearings, and expansion-joint gap size were considered in the analysis. The fragility curve was calculated for each bridge with 10 different selected far-fault records. The results showed that the bridge mass and friction coefficient of bearings have a significant effect on the seismic response.

Tubaldi et al. [12] concluded that the seismic response and vulnerability of self-consolidating concrete (SCC) bridges could exhibit dual load path result. A fully probabilistic approach was proposed to consider the input uncertainty for both record variability and the model parameters, incremental dynamic analysis (IDA) was used to propagate all pertinent sources of uncertainties to the seismic demand. The results showed that the response variability induced by model parameter uncertainty is significant.

Padgett and DesRoches [13] used gross geometries and far-fault ground motion variability to evaluate the modeling parameters which can affect the seismic response based on a retrofitted bridge sample. The results revealed the savings in simulation, computational effort, and the fragility estimation can be achieved through a preliminary screening of modeling parameters. However, the propagation of these potentially variable parameters tends to be dominated by the uncertainty in ground motion and structural geometry parameter.

Wang et al. [14] analyzed the uncertainty influence based on the fragility of bridges, where the uncertainty sources were concluded from recent collapsed bridge. The results showed that incorporating modeling uncertainties cannot only increase the dispersion in the fragility but also shift the median capacity of components to a smaller value. Since the key parameters can influence the design details in a uniform risk design framework, such impacts on the bridge fragility will further change the estimated risk level.

The above-cited studies were mainly focused on far-fault ground motions. Compared with far-fault ground motions, near-fault ground motions are considerably different as they are characterized by short duration, pulse-like ground motion (one or more pulses), significant vertical component, and different representative IM parameters [15–17]. Therefore, the seismic response and the probabilistic seismic demand model (PSDM) may be different.

In this paper, the effects of near-fault ground motions are applied to a regular continuous highway bridge to compare the IM parameters and establish the PSDM model for uncertainty parameter analysis; a specific distribution of uncertainty parameters concerning geometry, strength, mass, and damping ratio are selected for the calculation both in near-fault and far-fault conditions, the results are presented as the absolute difference ("swing") between the low and high values from each parameter distribution to draw the final tornado quantification diagram [18].

2 Bridge modeling and selected uncertainty range

2.1 Bridge modeling

This paper only considers regular highway bridges, whose seismic responses are basically controlled by fundamental vibration mode. The specific definition of regular highway bridges according to the Chinese Guidelines for Seismic Design of Highway Bridges [19] is reported in Table 1. Since the seismic response of a regular bridge is mainly controlled by fundamental vibration mode, it can be simplified as a single degree of freedom (SDOF) system, the pier and rubber bearings contribute to the stiffness

Table 1 Definition of regular bridges

design parameter	details and range				
span length	$\leqslant$90 m				
pier height	$\leqslant$30 m				
pier slenderness ratio	2.5–10				
number of spans	2	3	4	5	6
span-to-span length ratio	<3	<2	<2	<1.5	<1.5
column-to-column stiffness ratio	–	<4	<4	<3	<2
axial load ratio	<0.3				
bearing	rigidly connected, pin-connected, or supported on conventional bearings				
substructure	single-column pier, double-column pier, or multiple-column bent pier				
foundation condition	not susceptible to liquefaction, lateral spreading, or scour				

while the girder contribute to the mass in the longitudinal direction. In the transversal direction, shear keys are placed on the bent cap and abutments to restrict the transversal displacement of superstructure as usually the case in China.

A typical regular highway bridge is designed first according to the Chinese Guidelines for Seismic Design of Highway Bridges [19], and adopted as the prototype bridge in this study. The bridge is a three-span continuous PC girder bridge with span arrangement of 3 m × 20 m and width of 13.5 m. The hollow-slab girder and double-column piers are adopted in the bridge, and elastomeric pad bearings are placed on the cap beams of the piers. Each column of the piers has a circular cross section with a diameter of 1.2 m, and a height of 12 m. C30-grade concrete with a compressive strength of 30 MPa is used in the piers and C50-grade concrete with a compressive strength of 50 MPa is used in the girder. HRB335 rebar (f_{yk} = 335 MPa) and HPB 300 rebar (f_{yk} = 300 MPa) are used as the longitudinal and transverse reinforcement of the column, respectively. The longitudinal reinforcement ratio is 1.0% and the transverse one is 0.4% according to the Chinese Guidelines [19]. Capacity design method is adopted in seismic design of the bridge, and the piers are designed as ductile elements, while other components are designed as capacity protected elements.

The 3-dimensional finite element (FE) model of the prototype bridge is built using OpenSees software [20]. The aftershock data indicate that the bridge girder usually behaves elastically unless falling-off [21], so the hollow-slab girder is modeled using the elastic beam element. The bridge deck is simplified as lumped mass. Both the columns and the cap beams are modeled using nonlinear fiber beam-column element as shown in Fig. 1. The Kent-Scott-Park constitutive model is used for the concrete while the Giuffre-Menegotto-Pinto constitutive model is adopted for the reinforcement. Zero-length elastic spring elements are used to model the bearings between the girder and the cap beams. The abutments are assumed to follow a bilinear behavior after yielding, and the pile-soil effect is not considered in this study. The 3-dimensional FE model of the bridge is shown in Fig. 2. The numbers of total elements and nodes are 100 and 92, respectively.

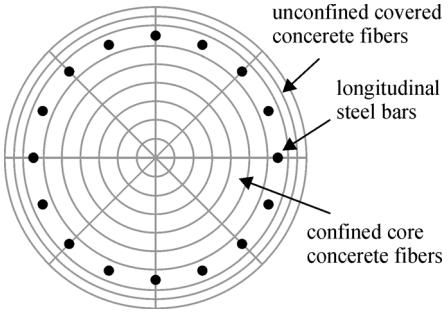

Fig. 1 Fiber element of the column.

2.2 Selected uncertainty range

The ultimate objective of the study is to quantify the significance during the seismic response analysis. To quantify the importance of different parameters, different sources of uncertainties that can affect both the structural seismic performance and demand are selected as the main influence factors; the details are listed as damping ratio (ξ), volume mass (m), pier diameter (D), longitudinal reinforcement diameter (d), concrete cover thickness (c), concrete compressive strength (f_c), and reinforcement yield strength (f_y).

Sources of uncertainty affecting structural performance are often characterized as either aleatory or epistemic. Aleatory uncertainty refers to inherent randomness, or stems from the unpredictable nature of events, whereas epistemic uncertainty is that which is due to a lack of knowledge, and stems from incomplete data, ignorance, or modeling assumptions. According to the related research and design codes, the selected uncertainty parameters are assumed as following given distribution as follows [22–25].

Under a strong ground motion, bridge structures will step into nonlinear behavior characterized with evident deformation, among which the input energy is primarily dissipated by the hysteretic displacement response. During the bridge modeling, damping ratio (ξ) is defined to help consider the energy dissipation mechanism. According to the Chinese Guidelines [19], the suggested damping ratio value for concrete structures is set as 0.05; during the modeling in OpenSees software, the Rayleigh damping is used with the combination of the structure mass and stiffness; according to the research of Nielson [26], the damping ratio of structures is assumed following normal distribution and the coefficient of variation (COV) is assumed as 30%.

In research of Chinese concrete volume mass difference and variability, the concrete volume mass (m) should follow a normal distribution [27], as for the specification of Chinese General Code for Design of Highway Bridges and Culverts [28], the suggested m value should range as 25–26 kN/m^3. On this basis, the volume mass of the girder and pier are assumed to follow a normal distribution, the mean value is set as 25.5 kN/m^3, and COV parameter of the normal distribution is set as 10% [29].

Geometry uncertainty parameters can also affect the nonlinear characteristics of the bridge structure, thus the pier diameter (D), the longitudinal reinforcement diameter (d), and the concrete cover thickness (c) are selected for the geometry uncertainty analysis following the normal distribution [30]. The mean values are selected from the original designed parameter, the COV of geometry parameters in the normal distribution are selected as 5%.

According to the Chinese Code for Design of Concrete Structures [31], the standard compressive strength of concrete C30 is fixed by the standard test method: after the

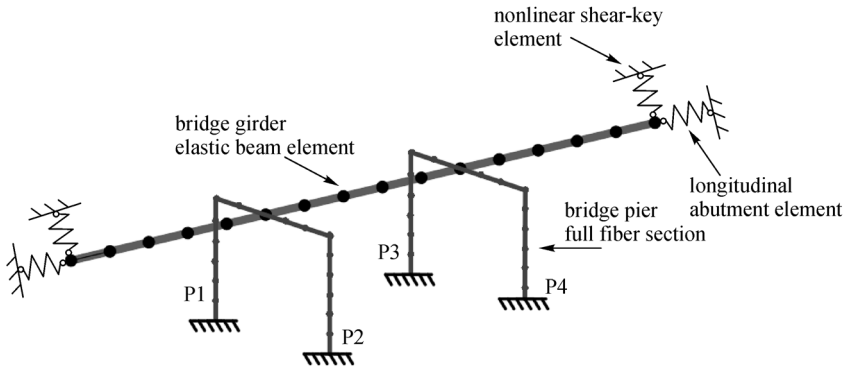

Fig. 2 3-dimensional FE model of the bridge.

cube specimens with side length of 150 mm are maintained for 28 days, the overall distribution of the compressive strength should be more than 95% as 30 MPa for the reliability; for the HRB335 longitude reinforcement, the standard yield strength value f_y and the mean yield strength value f_{ym} should satisfy the relationship as $f_y = (1-1.645\sigma_y)\ f_{ym}$ to ensure the 95% guaranteed rate for the design value, where the σ_y is the adjust coefficient. On these basis, the concrete compressive strength and the reinforcement yielding strength are assumed as lognormal distribution, the COV parameter of lognormal distribution for concrete and reinforcement strength are selected as 20% and 10%, respectively [32]. Figure 3 listed the selected uncertainty parameters and their related distribution detail; according to the distribution range and the COV parameter value, the low and high limit values are calculated based on the designed distribution setting as in Table 2.

3 Probabilistic seismic analysis for near-fault earthquake

After selecting the key sources of uncertainty parameters and their related distributions, a PSDM should be developed to offer the basis for quantifying the parameter significance [32]. Usually, the PSDM model is not only a key aspect for implementing the PBEE framework, but also the analysis basis for uncertainty parameters quantification. Generally, a PSDM model can be defined by a mathematical expression that correlates the IM parameter to a specific EDP parameter, and it can predict the value of the demand at a specific intensity value. Under the same IM parameter level, the influence of each uncertainty parameter can be compared with the fitting correlation result of the related EDP value.

The displacement drift ratio (*DR*) at the top of pier is selected as the EDP parameter in realistic measures of the bridge damage, which is correlated with the deformation ability for the piers under different performance level. The proposed EDP can consider the influences of slenderness ratio, axial load ratio, reinforcement ratio, stirrup ratio, and other design parameters [30]. In previous studies by the authors of this work, it was already found that in the far-fault domain, the peak ground acceleration (*PGA*) and DR at the top of pier follow a linear correlation relationship in natural logarithm coordinate system [33]. However, due to the special features and characters of the near-fault earthquake, more IM parameters should be discussed to obtain the ideal PSDM model for near-fault earthquake.

3.1 Ground motion selection

The site categories of the selected records are classified

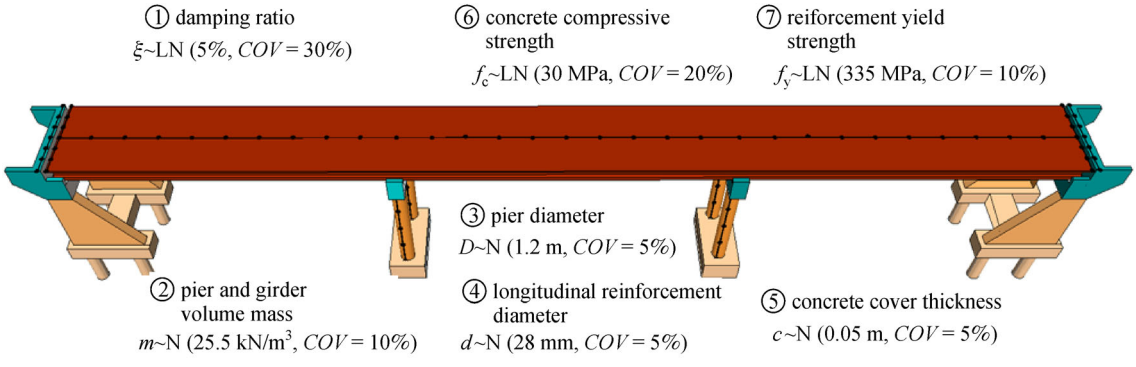

Fig. 3 Analytical model of regular highway bridge indicating probabilistic models of uncertain parameters.

Table 2 Modeling related parameters and the distribution value

No.	parameter	unit	distribution	mean values	COV	low limit	high limit
1	ξ	–	lognormal	5%	30%	2.53%	7.50%
2	m	kN/m^3	normal	25.5	10%	21.30	29.70
3	D	m	normal	1.2	5%	1.10	1.29
4	d	mm	normal	28	5%	25.70	30.30
5	c	m	normal	0.05	5%	0.046	0.054
6	f_c	MPa	lognormal	30	20%	20.13	39.90
7	f_y	MPa	lognormal	335	10%	279.90	390.10

based on the average shear wave velocity to a depth of 30m according to the Chinese guidelines for seismic design of highway bridges: type I ($V_{s30} > 510$ m/s), type II (260 m/s $< V_{s30} \leqslant 510$ m/s) and type III (150 m/s $< V_{s30} \leqslant 260$ m/s) [34]. All earthquake signals for near-fault and far-fault earthquake on 3 different site conditions are selected from the PEER ground motion database [35]. For better consider the effects of the vertical earthquake component, all the records are collected and input from vertical and horizontal direction with its original property. Since the number of near-fault earthquake records with significant velocity is quite limited, site condition IV is not considered at this step of research. Figure 4 shows the magnitude (*Mw*) and the fault distance (*R*) distribution for the inputs of near-fault on 3 site conditions, a total of 75 earthquake records are selected as the database. Each event of the selected near-fault earthquake record is marked with the characters of a significant pulse in the velocity time-history, ratio of peak ground velocity (*PGV*) to *PGA* larger than 0.15 and fault distance (*R*) within 20 km.

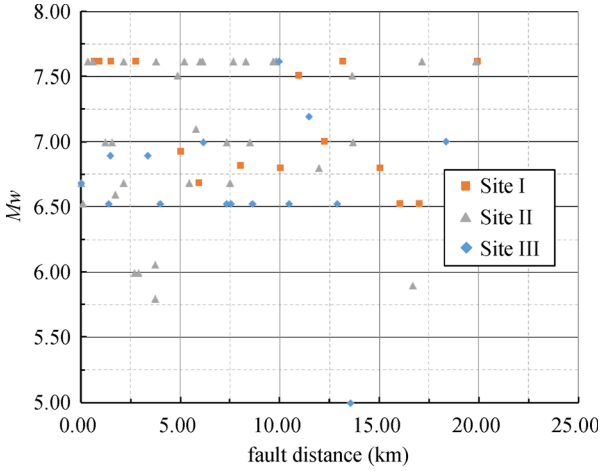

Fig. 4 Selected records for the probabilistic seismic analysis (Site I-15 records; Site II-35 records; Site III-15 records).

3.2 Near-fault PSDM

The chosen IMs are listed as *PGA*, *PGV*, *PGD*, the ratio of *PGV*/*PGA*, S_a, and predominant period, where *PGD* is the peak ground displacement, S_a is the spectral acceleration at the fundamental period with 5% damping, predominant period is the specific period when the maximum spectral energy is concentrated. The equations for the linear regression are also listed in Fig. 5, it shows that the *PGA*, *PGV*, *PGD*, and S_a have a positive fitting distribution with the bridge *DR*, whereas the *PGV*/*PGA* and predominant period show a negative fitting distribution. From the fitting result it can be concluded that *PGA* is the most correlated parameter for the bridge *DR* with the maximum determination coefficient R and the minimum standard deviation *P*.

Therefore, a PSDM for the bridge sample can be established. By selecting the *DR* and *PGA* as the parameters for EDP and IM, respectively, the linear regression formula obtained in this section can be applied to estimate the *DR* value as Eq. (1), where parameters *a* and *b* represent the slope and intercept of the fitting line as demonstrated in Fig. 6.

$$\ln(DR) = a\ln(PGA) + b. \tag{1}$$

Based on the analysis pre-settings, this PSDM model mainly focuses on the regular highway continuous bridges which are subjected to a near-fault earthquake with significant pulse at 3 different site conditions (Fig. 6). It can provide an estimation for the *DR* under the near-fault pulse-like records and offer a suitable fitting model for the uncertainty parameter analysis.

4 Uncertainty analysis of the prototype bridge

4.1 Selected IM

Given a certain IM parameter value, the significance of different uncertainty can be quantified by the EDP result base on the established PSDM model. In this section, the uncertainty analysis between the near-fault and far-fault earthquake are compared both in elastic and nonlinear cases. By selecting the *PGA* as the main IM parameter, with the accordance of Chinese seismic design code for urban bridges [36], the seismic design level can be divided into 2 levels by adjusting the *PGA* value: frequent

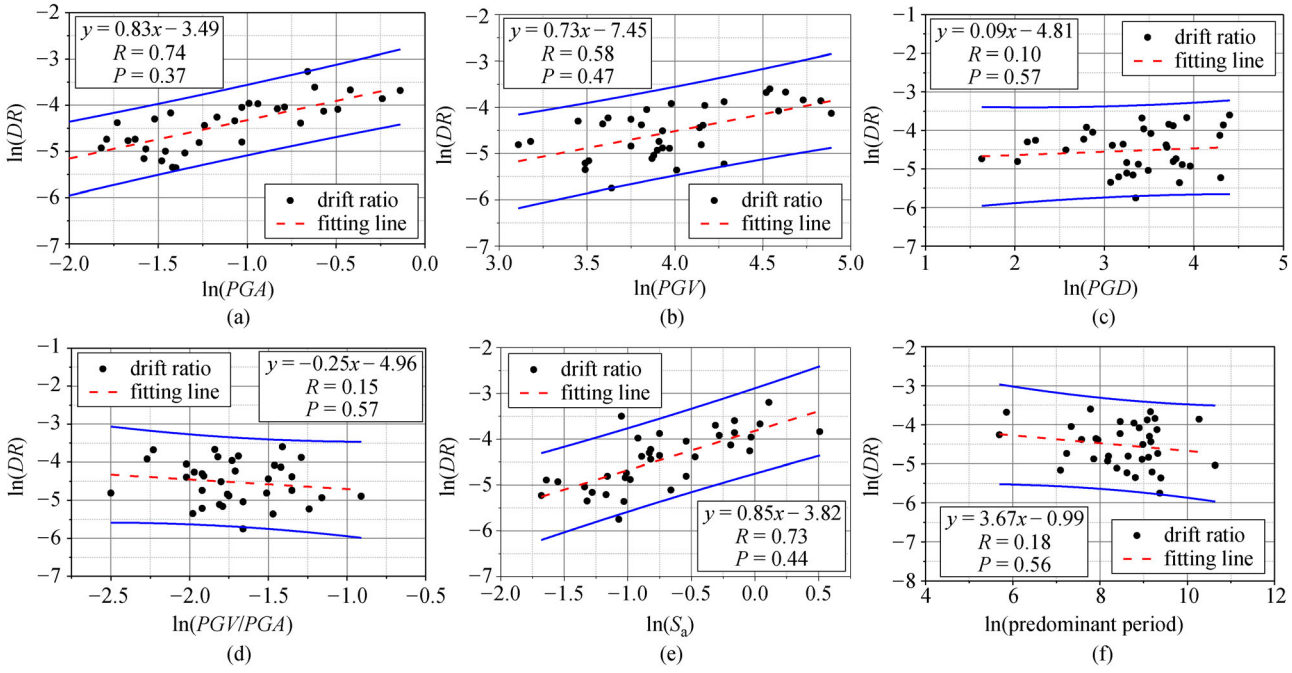

Fig. 5 Relationship between the *DR* and different IM parameter on the base of the results of the nonlinear analyses on bridge sample on site II condition: (a) *PGA*; (b) *PGV*; (c) *PGD*; (d) *PGV/PGA*; (e) S_a; (f) predominat period.

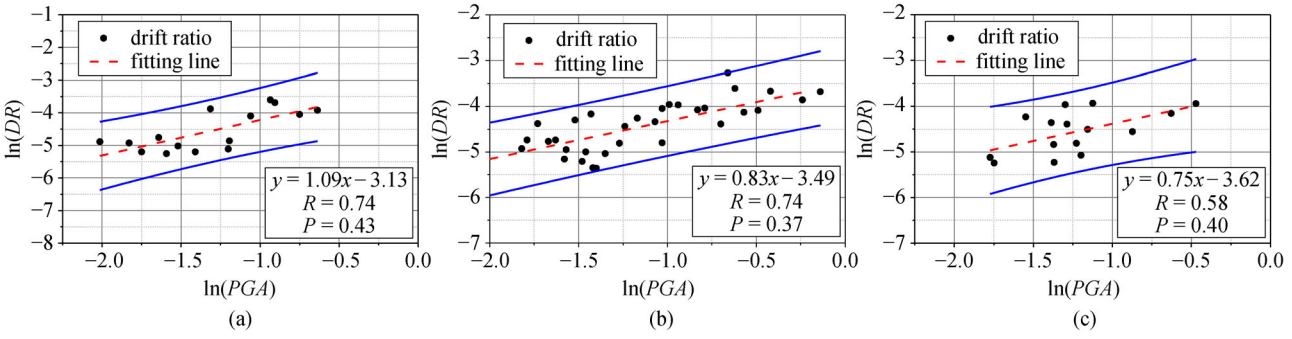

Fig. 6 Distribution of *DR* and *PGA* in natural logarithmic coordinate system on 3 different site condition: (a) Site I-15 records; (b) Site II-35 records; (c) Site III-15 records.

Table 3 Parameters of the selected seismic design level

seismic design level	earthquake type	return period (years)	evaluation statement	*PGA*
E1	frequent earthquake	475	elastic	0.05*g*
E2	rare earthquake	2500	inelastic	0.20*g*

earthquake evaluation (E1) and rare earthquake evaluation (E2). E1 corresponds to the earthquake with a Return Period of 475 years and E2 corresponds to the earthquake with a Return Period of 2500 years. The details of requirements are listed in Table 3. Levels of E1 and E2 evaluation are separately focused on the structure seismic response during the elastic and inelastic case. According to the Seismic Hazard Map of China, the uniform *PGA* value for E1 and E2 are, respectively, 0.05*g* and 0.20*g*. For providing enough fitting accuracy, a total of 90 earthquake records are selected from the PEER ground motion database considering both near-fault and far-fault records on 3 site conditions to ensure calculation accuracy.

Figure 7 shows the magnitude (*Mw*) and the fault distance (*R*) distribution results for the uncertainty influence analysis, it consider both the near-fault and far-

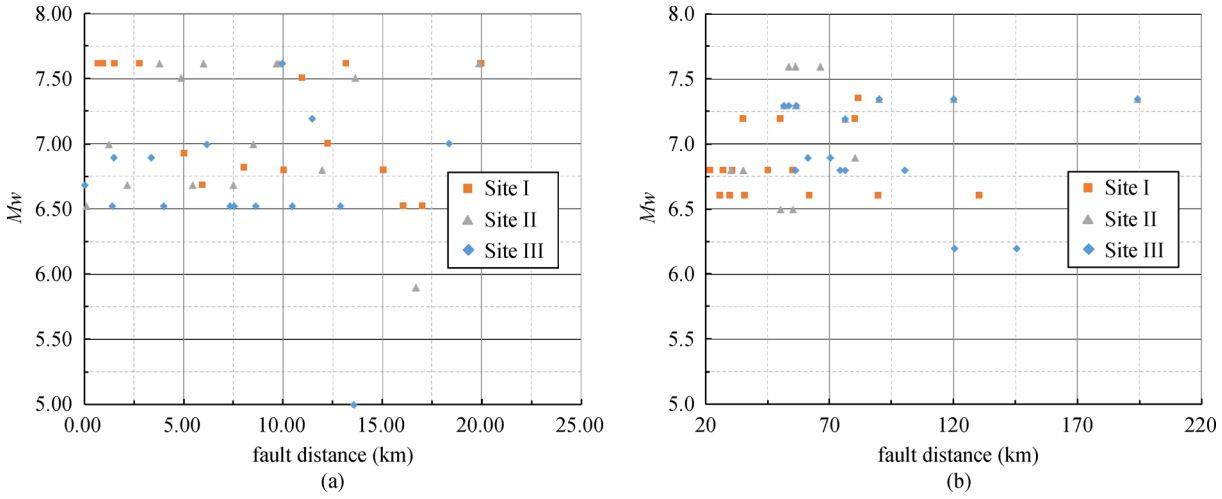

Fig. 7 Selected records for the damage mechanism comparison: (a) near-fault records; (b) far-fault records (Site I-15 records; Site II-15 records; Site III-15 records).

fault cases, the select criterion of the near-fault earthquake records remains similar as in Fig. 5, which ensure the significant pulse during the velocity time-history, a total of 90 earthquake records are selected as the analysis database.

4.2 Quantification of uncertainties

After the establishment of the PSDM model and IM level, the influence of different uncertainty parameters can be quantified. Among different global sensitivity analysis approaches, the Morris One-At-a-Time (MOAT) method is suitable for the linear regression result. Morris [37] first presented the concept of elementary effects in 1991 as the derivatives over the space of parameters. This method is a simple but effective global method for screening a few important input parameters. The total effect and interaction effect for each parameter on the output can be described by the mean μ and standard deviation σ.

During the uncertainty analysis, all parameters of the finite element model were first set equal to their respective mean values to carry the time-history analysis. Subsequently, each parameter was changed to the limit value separately and submitted to the original one for comparison. The absolute result difference of the low and high limit values from the parameter distribution is called the "swing" which can contribute to the tornado diagram as the final judgement [38]. Based on the swing difference of uncertainty parameters at 3 different site conditions with near-fault and far-fault cases, the tornado diagrams are listed as follows where μ is the mean value of 15 calculation results and the σ is the standard deviation of the fitting results.

4.2.1 E1 Case

The quantification results of the uncertainties under E1 level at 3 different site conditions are present as Figs. 8–10. From the tornado distribution diagram, a few conclusions can be concluded: the distributions of μ-swing act as the similar pattern with the σ-swing; parameters of ξ, D, and f_c are the most effective uncertainty parameters for both near-fault and far-fault at 3 site conditions with a large swing value; when compare to the near-fault, the swing results of the far-fault are quite similar; the differences of the μ-swing at 3 site conditions are not significant and the

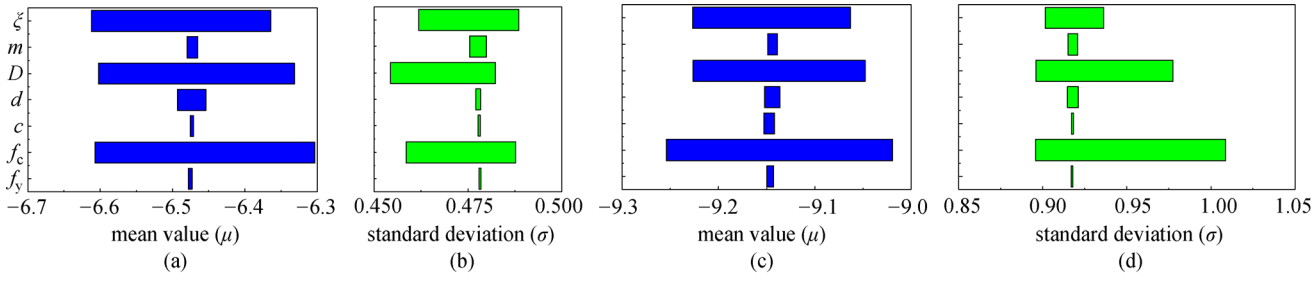

Fig. 8 Tornado diagrams for the example bridge on site condition I (NF-Near-fault, FF-Fault fault). (a) NF-μ; (b) NF-σ; (c) FF-μ; (d) FF-σ.

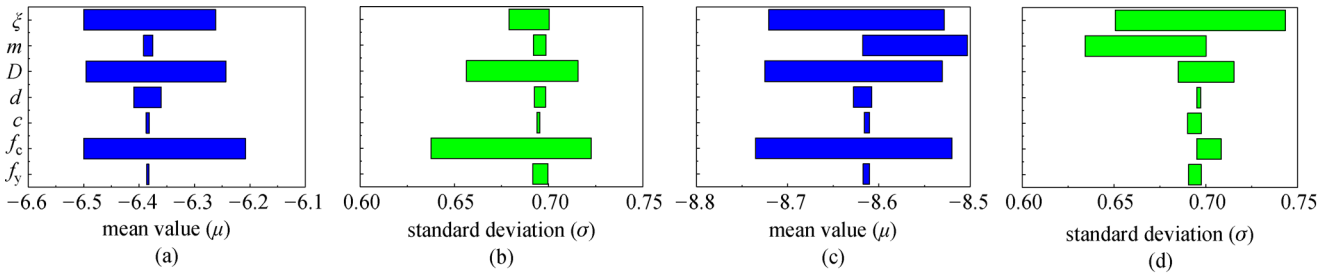

Fig. 9 Tornado diagrams for the example bridge on site condition II (NF-Near-fault, FF-Fault fault). (a) NF-μ; (b) NF-σ; (c) FF-μ; (d) FF-σ.

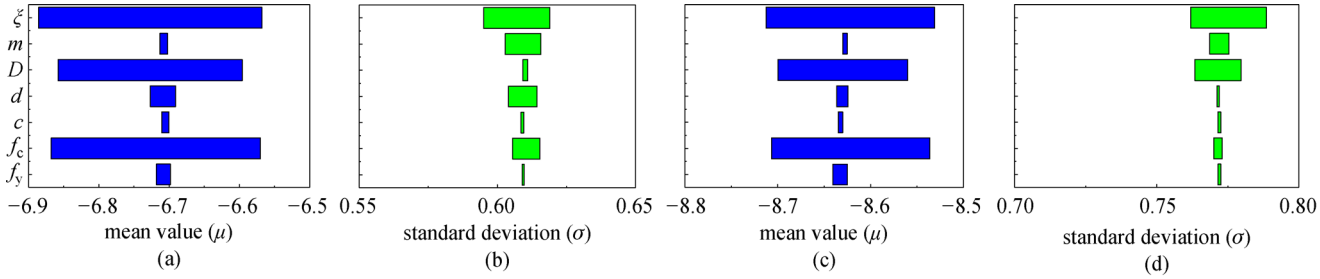

Fig. 10 Tornado diagrams for the example bridge on site condition III (NF-Near-fault, FF-Fault fault). (a) NF-μ; (b) NF-σ; (c) FF-μ; (d) FF-σ.

σ-swing on site condition III correspond with the minimum value.

4.2.2 E2 Case

The quantification results of the uncertainties under E2 level on 3 site conditions are present as Figs. 11–13, from the tornado distribution diagram, it can be concluded that when compared with E1 level, the significance degree among the uncertainty parameters is more clear under the near-fault case; as to the near-fault earthquake, ξ is the most significant uncertainty parameter with the related distinctive swing difference; when compared with the far-fault ground motion, the near-fault correspond with smaller but more clear distinguish swing value; the uncertainty swing difference of far-fault among 3 site conditions is not significant.

Through the uncertainty quantification it can be concluded that: the parameter uncertainties of ξ, D, and f_c are all significant for both near-fault and far-fault earthquake at two seismic evaluation levels, however the near-fault earthquake show a better distinguish result for quantifying the influence degree of different uncertainties; the parameter uncertainties of m, d, c, and f_c have a weaker influence according to the quantification results.

5 Conclusions

The main purpose of this study is to establish a PSDM for regular highway continuous bridge under the near-fault ground motion and quantify the significance of different modeling uncertainty parameters during the seismic analysis. The results of this study demonstrate that:

1) *PGA* is a proper IM parameter for establishing the PSDM model for regular highway continuous bridges both in near-fault and far-fault earthquake cases.

2) In natural logarithm coordinate, the PSDM of PGA and the *DR* follow a linear distribution relationship.

3) The damping ratio, pier diameter and the concrete

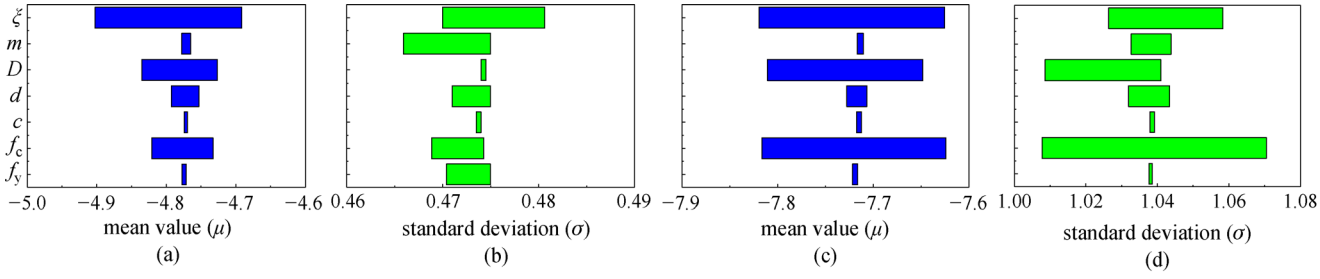

Fig. 11 Tornado diagrams for the example bridge on site condition I. (a) NF-μ; (b) NF-σ; (c) FF-μ; (d) FF-σ.

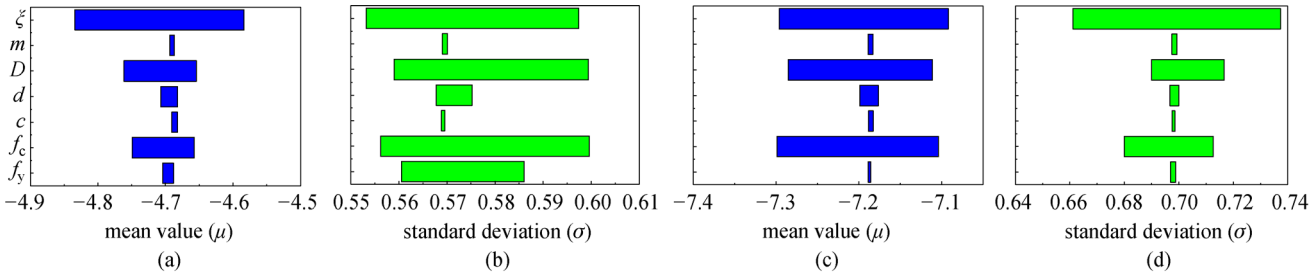

Fig. 12 Tornado diagrams for the example bridge on site condition II. (a) NF-μ; (b) NF-σ; (c) FF-μ; (d) FF-σ.

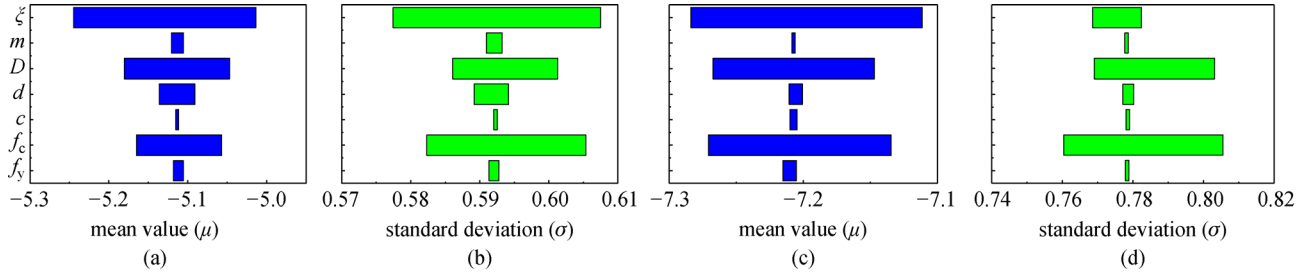

Fig. 13 Tornado diagrams for the example bridge on site condition III. (a) NF-μ; (b) NF-σ; (c) FF-μ; (d) FF-σ.

strength are the significant uncertainty parameters for both near-fault and far-fault earthquake cases at two seismic design levels. Damping ratio acquired the maximum significant result under the near-fault earthquake with the E2 seismic design level.

4) Ongoing work is focused on more advanced stochastic modeling and uncertainty quantification methods to increase the result accuracy.

Acknowledgements This work was supported by the Poliba2China Project Funding (Italy Code Number: CUPD96D17000110002), and the National Natural Science Foundation of China (Grant No. 51878180), and the Transportation Science and Technology Development Project of Fujian Province (No. 201803).

References

1. SEAOC. Vision 2000: Performance Based Seismic Engineering of Buildings. Sacramento, CA: Structural Engineers Association of California, 1995
2. Fan L C. Life cycle and performance based seismic design of major bridges in China. Frontiers of Architecture and Civil Engineering in China, 2007, 1(3): 261–266
3. Ghobarah A. Performance-based design in earthquake engineering: State of development. Engineering Structures, 2001, 23(8): 878–884
4. Deierlein G G, Krawinkler H, Cornell C A. A framework for performance-based earthquake engineering. In: Proceedings of 2003 Pacific Conference on Earthquake Engineering. Christchurch: New Zealand Society for Earthquake Engineering, 2003
5. Porter K A. An overview of PEER's performance-based earthquake engineering methodology. In: Proceedings of the 9th International Conference on Applications of Statistics and Probability in Civil Engineering. San Francisco: Civil Engineering Risk and Reliability Association, 2003
6. Moehle J, Deierlein G G. A framework methodology for performance-based engineering. In: Proceedings of the 13th World Conference on Earthquake Engineering. Vancouver B C: Canadian Association for Earthquake Engineering, 2004: 1–13
7. Porter K A, Beck J L, Shaikhutdinov R V. Sensitivity of building loss estimates to major uncertain variables. Earthquake Spectra, 2002, 18(4): 719–743
8. Vu-Bac N, Silani M, Lahmer T, Zhuang X, Rabczuk T. A unified framework for stochastic predictions of mechanical properties of polymeric nanocomposites. Computational Materials Science, 2015, 96: 520–535
9. Vu-Bac N, Lahmer T, Keitel H, Zhao J, Zhuang X, Rabczuk T. Stochastic predictions of bulk properties of amorphous polyethylene based on molecular dynamics simulations. Mechanics of Materials, 2014, 68: 70–84
10. Vu-Bac N, Lahmer T, Zhuang X, Nguyen-Thoi T, Rabczuk T. A software framework for probabilistic sensitivity analysis for computationally expensive models. Advances in Engineering Software, 2016, 100: 19–31
11. Pan Y, Agrawal A K, Ghosn M. Seismic fragility of continuous steel highway bridges in New York state. Journal of Bridge Engineering, 2007, 12(6): 689–699
12. Tubaldi E, Barbato M, Dall'asta A. Influence of model parameter uncertainty on seismic transverse response and vulnerability of steel-concrete composite bridges with dual load path. Journal of Structural Engineering, 2012, 138(3): 363–374
13. Padgett J E, DesRoches R. Sensitivity of seismic response and fragility to parameter uncertainty. Journal of Structural Engineering, 2007, 133(12): 1710–1718
14. Wang Z, Padgett J E, Dueñas-Osorio L. Toward a uniform risk

design philosophy: Quantification of uncertainties for highway bridge portfolios. In: Proceeding of the 7th National Seismic Conference on Bridges & Highways. Oakland: Multidisciplinary Center for Earthquake Engineering Research, 2013

15. Somerville P G, Smith N F, Graves R W, Abrahamson N A. Modification of empirical strong ground attenuation relations to include the amplitude and duration effects of rupture directivity. Seismological Research Letters, 1997, 68(1): 199–222
16. Niazi M, Bozorgnia Y. Behaviour of near-source peak vertical and horizontal ground motions over SMART-1 array, Taiwan. Bulletin of the Seismological Society of America, 1991, 81(3): 715–732
17. Chopra A K, Chintanapakdee C. Comparing response of SDOF systems to near-fault and far-fault Earthquake motions in the context of spectral regions. Earthquake Engineering & Structural Dynamics, 2001, 30(12): 1769–1789
18. Porter K A, Beck J L, Shaikhutdinov R V. Sensitivity of building loss estimates to major uncertain variables. Earthquake Spectra, 2002, 18(4): 719–743
19. Ministry of Communications of the People's Republic of China. Guidelines for Seismic Design of Highway Bridges (JTG/T B02–01–2008). Beijing: People's Communications Press, 2008 (in Chinese)
20. Mazzoni S, McKenna F, Scott M, Fenves G. Open System for Earthquake Engineering Simulation (OpenSees), User Command Language Manual. Berkeley: Pacific Earthquake Engineering Research Center, University of California, 2006
21. Hambly E C. Bridge Deck Behavior. 2nd ed. New York: Van Nostrand Reinhold, 1991
22. Hamdia K M, Silani M, Zhuang X, He P, Rabczuk T. Stochastic analysis of the fracture toughness of polymeric nanoparticle composites using polynomial chaos expansions. International Journal of Fracture, 2017, 206(2): 215–227
23. Hamdia K M, Ghasemi H, Zhuang X, Alajlan N, Rabczuk T. Sensitivity and uncertainty analysis for flexoelectric nanostructures. Computer Methods in Applied Mechanics and Engineering, 2018, 337: 95–109
24. Vu-Bac N, Lahmer T, Zhang Y, Zhuang X, Rabczuk T. Stochastic predictions of interfacial characteristic of polymeric nanocomposites (PNCs). Composites. Part B, Engineering, 2014, 59: 80–95
25. Vu-Bac N, Rafiee R, Zhuang X, Lahmer T, Rabczuk T. Uncertainty quantification for multiscale modelling of polymer nanocomposites with correlated parameters. Composites. Part B, Engineering, 2015, 68: 446–464
26. Nielson B, Desroches R. Analytical seismic fragility curves for typical bridges in the central and south-eastern United States. Earthquake Spectra, 2007, 23(3): 615–633
27. Yu X H. Probabilistic seismic fragility and risk analysis of reinforced concrete frame structures. Dissertation for the Doctoral Degree. Harbin: Harbin Institute of Technology, 2012 (in Chinese)
28. The Ministry of Communications of the People's Republic of China. General Code for Design of Highway Bridges and Culverts, JTG D60. China Beijing: Communications Press, 2004 (in Chinese)
29. Wu W P. Seismic fragility of reinforced concrete bridges with consideration of various sources of uncertainty. Dissertation for the Doctoral Degree. Changsha: Hunan University, 2016 (in Chinese).
30. Padgett J E, Nielson B G, Desroches R. Selection of optimal intensity measures in probabilistic seismic demand models of highway bridge portfolios. Earthquake Engineering & Structural Dynamics, 2008, 37(5): 711–725
31. National Standard of the People's Republic of China. GB 50010–2010. Code for Design of Concrete Structures. Beijing: China Architecture and Building Press, 2010 (in Chinese)
32. Pang Y T, Wu X, Shen G Y, Yuan W C. Seismic fragility analysis of cable-stayed bridges considering different sources of uncertainties. Journal of Bridge Engineering, 2014, 19(4): 04013015
33. Ma H B, Zhuo W D, Yin G, Sun Y, Chen L B. A probabilistic seismic demand model for regular highway bridges. Applied Mechanics and Materials, 2016, 847: 307–318
34. Lv H S, Zhao F X. Site coefficients suitable to China site category. Earth Science, 2007, 29(1): 67–76
35. Chiou B, Darragh R, Gregor N, Silva W. NGA project strong-motion database. Earthquake Spectra, 2008, 24(1): 23–44
36. Chinese Ministry of Housing and Urban Rural Development. Code for Seismic Design of Urban Bridges, CJJ 166–2011. Beijing: China Architecture and Building Press, 2011 (in Chinese)
37. Morris M D. Factorial sampling plans for preliminary computational experiments. Technometrics, 1991, 33(2): 161–174
38. Porter K A, Beck J L, Shaikhutdinov R V. Sensitivity of building loss estimates to major uncertain variables. Earthquake Spectra, 2002, 18(4): 719–743